DRAG REDUCTION BY COOLING IN HYDROGEN FUELED AIRCRAFT

Eli Reshotko*
Case Western Reserve University
Cleveland, Ohio 44106, U.S.A.

ABSTRACT

Drag reductions are possible for cryo-fueled aircraft by using the fuel to cool selected aerodynamic surfaces on its way to the engines. This is because cooled laminar boundary layers in air at subsonic and low supersonic speeds are more stable than adiabatic boundary layers and therefore more resistant to transition to turbulent flow. Calculations for a M = 0.85 hydrogen-fueled transport show that drag reductions in cruise of about 20% are within reason. The weight of the fuel saved is well in excess of the weight of the required cooling system. These results suggest that the hydrogen-fueled aircraft employing surface cooling is quite attractive as an energy conservative aircraft and warrants more detailed study.

INTRODUCTION

Brewer[1] argues quite convincingly that hydrogen-fueled aircraft can satisfactorily handle the needs of air transportation when petroleum fuels are no longer consistently available. Hydrogen however is not the only alternative to petroleum fuels. Mikolowsky, Noggle and Stanley[2] rate propulsion system options for very large transport aircraft using different alternative fuels on the basis of cost and energy effectiveness for a variety of scenarios. They indicate a preference for a propulsion system using synthetic JP rather than cryo-fueled or nuclear options. They show nevertheless that for many missions the liquid methane (LCH_4) and liquid hydrogen (LH_2) aircraft are only marginally less effective than the aircraft fueled by synthetic JP.

A factor not considered by either Brewer[1] or Mikolowsky et al[2] is the drag reduction that might be obtained by using the cryo-fuel (LCH_4 or LH_2) to cool major aerodynamic surfaces of the aircraft as it flows from the fuel tanks to the engines. Cooled laminar boundary layers in air at subsonic and low supersonic speeds are more stable than adiabatic boundary layers and are therefore more resistant to transition to turbulent flow. Thus one has the prospect of laminarization by cooling with the consequent reduction in skin friction drag.

This paper will examine the aerodynamic basis for drag reduction by cooling in subsonic flight. This information will then be applied to the example of a M = 0.85 hydrogen-fueled transport in cruise. Some comments will be made on cooling system design and the effects of drag reduction and cooling system weight on fuel saving.

*Professor of Engineering, Fellow AIAA

AERODYNAMICS OF DRAG REDUCTION BY COOLING

Since drag reduction by cooling depends on the delay of transition that comes about through cooling, one must first examine the effect of cooling on stability and transition of subsonic boundary layers in air. The prospects for cooling depend further on whether the cooling capacity of the fuel can cool the aircraft skin down to the temperatures needed for the desired transition delay. These two factors are examined in this section.

Stability and Transition

Boundary layers on aircraft surfaces display some three-dimensionality, that is that the velocity vectors within the boundary layer are not all in the direction of the local free-stream. In principle this requires that the stability of the three-dimensional compressible boundary layers be analyzed in a proper three-dimensional way. Such an analysis is not yet available although there have been significant advances recently for incompressible three-dimensional boundary layers[3-6]. Unfortunately the incompressible procedures do not lend themselves to considering the effects of cooling. Srokowsky and Orszag[5] and Mack[6] do however show that when the crossflow is unstable, the overall three-dimensional stability characteristics are very close to those of the crossflow alone and when the crossflow is small enough to be stable, the stability characteristics are essentially those of the streamwise flow. Thus for the purposes of this paper we can establish the trends of the effects of cooling on stability by reverting to the traditional procedure whereby the stability of the streamwise and crossflow velocity profiles are separately considered.

Effect of Cooling on Stability and Transition of Streamwise Flows - It was noted many years ago in experiments at low subsonic speeds[7,8] that the transition location of the flat plate boundary layer in air is advanced as a result of plate heating. This trend was confirmed by the stability calculations of Lees[9] who showed that cooling can significantly stabilize the flat plate

boundary layer while heating destabilizes the boundary layer.

These results are shown in Figure 1 where length Reynolds number is plotted against the wall to free-stream static temperature ratio. The transition data of Frick and McCullough[7] and Liepmann and Fila[8] both show the decreasing transition Reynolds number with heating*. The difference in level reflects difference in the pressure gradients on the models as well as differences in quality of the test facilities. All the other curves in Figure 1 are of minimum critical Reynolds number -- that Reynolds number below which all small disturbances in a boundary layer are damped. Lees' result for M = 0.7 was obtained by an approximate asymptotic procedure. Shown also are the much more recent results of Boehman and Mariscalco[10] for M = 0.6 and M = 0.9 on a flat plate obtained by exact numerical solution of the compressible disturbance equations. Note the steep increase in minimum critical Reynolds number with cooling. If the wall is cooled to 0.7 T_e, the minimum critical Reynolds numbers for flat plate boundary layers are above 10^7 and the transition Reynolds number are even higher. The favorable pressure gradients typical of airfoils and fuselages tend to further increase both the minimum critical and transition Reynolds numbers.

Some experimental support is available for the aforementioned stability trends. Kachanov, Koslov and Lecvhenko[11] have observed a doubling of the minimum critical Reynolds number by cooling a flat plate in low speed flow to 0.945 T_e, confirming expectations from the calculations of Gaponov and Maslov[12]. These results are also shown in Figure 1. Kachanov et al[11] also measured the growth rates of the uncooled and cooled boundary layers for a range of frequencies. The neutral points (zero growth rate) are shown in Figure 2. For the uncooled boundary layer, their results are in agreement with prior experiments[13-15]. With cooling, not only does the minimum critical Reynolds number increase but the range of amplified frequencies is diminished. Furthermore, at a particular frequency that displays growth with and without cooling, the growth with cooling is much below that for the uncooled boundary layer (Figure 3). Thus, cooling clearly stabilizes the boundary layer in air at subsonic speeds and delays the onset of transition.

The estimation of transition Reynolds number for the streamwise flow is however another matter. The transition Reynolds number is demonstrably a function of the steady flight parameters alone. Nevertheless some success in transition estimation was demonstrated by Smith and Gamberoni[16] and by van Ingen[17]. For low speed flow, they correlated transition Reynolds numbers over plates, wings and bodies with the amplitude of the most unstable frequency from its neutral point to the transition point. Smith and Gamberoni[16] found that the transition Reynolds number $Re_{x_{tr}}$ as predicted by assuming an amplification factor of e^9 was seldom in error by more than 20%. Even if this criterion is fundamentally deficient it can certainly help evaluate the relative tendency to transition of a related set of flows. Most interesting is the result of Wazzan and Gazley[18] for water boundary layers (Figure 4) that minimum critical Reynolds numbers and transition Reynolds numbers based on e^9 correlate very well with the form factor $H \equiv \delta^*/\theta$ for pressure gradient, heating* or combinations of the two. Implied by this figure is a fairly good correlation of transition Reynolds number with minimum critical Reynolds number for low speed variable property flows.

A schedule of transition Reynolds number with surface temperature will be needed for later calculations. Figure 5 shows a plot of minimum critical Reynolds number for M = 0.85 as interpolated from Boehmann and Mariscalco[10] and the corresponding variation of transition Reynolds number obtained using Figure 4. Again, this schedule is for a flat plate and does not consider effects of the favorable pressure gradients found on forward portions of wings and bodies.

Crossflow Instability and Transition - Despite the great interest in crossflow instability, there are no calculations available for cooled boundary layers, so that it is not possible to establish definitive trends for the effects of cooling on the stability of crossflow boundary layers. There is some suspicion that cooling will not affect crossflow stability as much as it affected the stability of the streamwise flow since the crossflow velocity profile has an inherent inflectional character. Nevertheless cooling tends to decrease the maximum cross-flow velocity[20] which promotes increased cross-flow stability.

In the absence of anything more definitive, the cross-flow instability will be examined in terms of the χ criterion originally introduced by Owen and Randall[21]:

$$\chi = \frac{1}{\nu} \int_0^\infty W \, dy \qquad (1)$$

The quantity χ which is well known in LFC technology has the character of a thickness Reynolds number where the characteristic velocity is the average velocity of the cross-flow profile. If χ is kept below a certain critical value, transition can be avoided. Referring to Figure 6, the cross-flow velocity profile can be written

$$W = u_e \sin\theta \, (f'-g) \qquad (2)$$

*For the Frick and McCullough data, the upper point at $T_w/T_e = 1.14$ is for heat applied only ahead of the pressure minimum while for the lower point, heat is applied over the entire laminar flow. The upper and lower curves of the Liepmann and Fila data are for free-stream turbulence levels of 0.05% and 0.17% respectively.

*Boundary layers in water are stabilized by heating. Just as cooling in air reduces the viscosity, heating of liquids reduces their viscosities. A reduced viscosity near the wall requires larger velocity gradients to maintain the same level of shear stress. This promotes fuller velocity profiles which are more stable than velocity profiles over adiabatic walls. A significant reduction of drag is available to water vehicles with on-board propulsion systems if the reject heat of the propulsion system is discharged through heating the laminar flow portion of the hull[19].

where

$$f' = \frac{u}{u_e} \qquad g = \frac{w}{w_e}$$

u_e and w_e are respectively the chordwise and spanwise components of the local freestream velocity vector and θ is the angle between the local freestream velocity vector and the chordwise direction. Assuming for simplicity that the boundary develops according to local similarity and with constant properties, the expression for χ can be written:

$$\chi = \sqrt{\frac{2}{\nu}\left(\int_o^x u_e dx\right)} \quad \sin\theta \quad \left[\int_o^\infty (f'-g)d\eta\right]_\beta \qquad (3)$$

This expression has three factors, (a) the square root of the length Reynolds number, (b) $\sin\theta$ which in the region of interest is approximately $\sin\Lambda$, and (c) a profile integral which is a function of the local pressure gradient parameter β given by:

$$\beta = \frac{2}{u_e^2}\left(\frac{du_e}{dx}\right)\int_o^x u_e dx \qquad (4)$$

A flat plate has no crossflow. With pressure gradient the chordwise and spanwise profiles differ yielding the variation of the profile integral shown in Figure 7. This figure is based on the boundary layer computations of Beckwith[22]. Cooling the wall to 0.75 of the stagnation temperature reduces this factor by about 15%.

As indicated by equation (3), χ can be kept small by reducing sweep angle and by coming to zero pressure gradient within a short distance downstream of the attachment line. The supercritical airfoil sections (Figure 8) lend themselves to minimizing the possibility of crossflow transition. For the pressure distribution shown, critical regions are within the first 10% of chord, downstream of 75% chord on the upper surface and downstream of 55% chord on the lower surface. Much of the wing beyond 75% chord is taken up with movable control surfaces which would be very complicated to cool. If one wishes to laminarize only 75% of the wing, then the major area of concern for crossflow transition is near the attachment line.

It should be mentioned that suction is quite effective in quenching crossflow instability. If the design demands, some suction can be applied in the vicinity of the attachment line.

It should be very clear that compressible crossflow instability must be studied theoretically and possibly experimentally in order to properly evaluate the potential of cooling in quenching this instability.

Leading Edge Contamination - For a swept wing attached to a fuselage, turbulent flow from the fuselage can spread along the wing stagnation or "attachment" line. Such contamination can also occur if the spanwise flow at the attachment line is tripped by excessive surface roughness. Pfenninger and Reed[23] indicate that when there are large leading edge disturbances, this leading edge or spanwise contamination occurs when the momentum thickness Reynolds number on the attachment line $Re_{\theta_{a.\ell.}}$ ($Re_{\theta_{a.\ell.}} = w_\infty\theta/\nu$ where θ is the momentum thickness of the laminar spanwise boundary layer along the attachment line) is greater than 90 or 100. If the attachment line flow is kept relatively clean by fences or root suction, laminar flow could be maintained to $Re_{\theta_{a.\ell.}}$ up to 200-240.

A recent study by Poll[24] confirmed these findings. Poll's results for an RAE 101 airfoil at flight conditions are shown in Figures 9-11. His parameter ϕ is identical to $Re_{\theta_{a.\ell.}}$. It is seen that leading edge contamination can be avoided by shielding the attachment line flow from disturbances, reducing sweep angle and leading edge radius.

The effect of cooling on these criteria is not known. However difficulties in maintaining laminar attachment line flow can also be overcome by suction along the attachment line. This suction if used will also help a bit with crossflow instability.

Aerodynamic Heating and Friction Drag

On the premises that leading edge contamination and crossflow instability can be avoided and that laminar flow can be maintained according to a schedule such as that of Figure 5, it is of interest to determine the extent to which the cryo-fuel can in fact cool the aerodynamic surfaces. The aircraft components subject to drag reduction by cooling are the wings, the fuselage, the engine pods (nacelles), and the horizontal and vertical tail surfaces.

Heat Balance - A heat balance relation can be written for each aircraft component as follows:

$$(Mc)\frac{dT_w}{dt} = Q_{aero} - \dot{m}_f \Delta h_{T_w} \qquad (5)$$

where (Mc) is the heat capacity of the component, $\dot{m}_f$ is the fuel rate to the component and $(\Delta h)_{T_w}$ is the enthalpy increase of the fuel in going from its storage temperature to T_w. The aerodynamic heating term for a given component can be written

$$Q_{aero} = \rho_e u_e c_p \frac{Pr^{-2/3}}{z} A_w \left\{(C_{F_\ell})_{lam}(T_{aw}-T_w)_{lam}\sqrt{\frac{x_{tr}}{\ell}} + (C_{F_\ell})_{turb}(T_{aw}-T_w)_{turb}\left[1-\left(\frac{x_{tr}}{\ell}\right)^{6/7}\right]\right\} \qquad (6)$$

where the fluid properties are those of air at altitude, ℓ is the length of the section to be cooled, A_w is the wetted area to length ℓ, x_{tr} is the transition location at temperature T_w, and $(C_{F_\ell})_{lam}$ and $(C_{F_\ell})_{turb}$ are the respective laminar and turbulent average friction coefficient for length ℓ. For a flat plate for example

$$(C_{F_\ell})_{lam} = \frac{1.328}{\sqrt{\frac{u_e \ell}{\nu}}} \qquad (7)$$

$$(C_{F_{\ell\ turb}}) = \frac{0.0303}{(\frac{u_e \ell}{\nu})^{1/7}} \qquad (8)$$

Cooldown of a component can occur only if the cooling capacity of the fuel exceeds the aerodynamic heating, that is when the right side of equation (5) is negative.

It is of interest at this point to compare the cooling capacilities of hydrogen and methane. These fuels would be stored at pressures between one and two atmospheres. Figure 12 shows the enthalpy above that at saturated liquid conditions as a function of temperature at one atmosphere for the two fuels. The enthalpy difference for methane is considerably less than that for hydrogen. However, since the heat of combustion of methane is only about 40% that of hydrogen, the methane fuel rate would be about 2.5 times that for hydrogen for the same application. The broken line shows the "adjusted" methane capability relative to hydrogen. At wall temperatures of the order of 300°R, methane provides about 70% of the cooling capability of hydrogen.

Frictional Drag - The frictional drag coefficient of an aerodynamic component of overall length L and with transition located at x_{tr} is

$$C_{D_F} = (C_{D_F})_{lam} \sqrt{\frac{x_{tr}}{L}} + (C_{D_F})_{turb} \{1-(\frac{x_{tr}}{L})^{6/7}\} \qquad (9)$$

where $(C_{D_F})_{lam}$ and $(C_{D_F})_{turb}$ are the respective laminar and turbulent frictional drag coefficients for length L. They are referenced to the wing area, S, as is appropriate for aircraft drag coefficients. When the entire cooled length ℓ is laminar, then

$$C_{D_F} = (C_{D_F})_{lam} \sqrt{\frac{\ell}{L}} + (C_{D_F})_{turb} \{1-(\frac{\ell}{L})^{6/7}\} \qquad (10)$$

and the drag saving is

$$\Delta C_{D_F} = (C_{D_F})_{turb} - C_{D_F}$$

$$= [(C_{D_F})_{turb} (\frac{\ell}{L})^{6/7} - (C_{D_F})_{lam} \sqrt{\frac{\ell}{L}}] \qquad (11)$$

FEASIBILITY OF DRAG REDUCTION BY COOLING FOR A M = 0.85 LARGE TRANSPORT AIRCRAFT

The aircraft used in this study is a conceptual design for a hydrogen fueled transport developed by Brewer[25] et al. The design has the appearance of a conventional wide-bodied transport except for a larger fuselage to accommodate the liquid hydrogen storage tanks (Figure 13). It has a design range of 5500 n.mi with a payload of 400 passengers. The aircraft is assumed to cruise at 37,000 ft.

The drag breakdown in cruise for the aircraft without cooling assuming turbulent boundary layers is

Drag Component		Drag Coefficient	% of Total
Induced Drag	C_{D_i}	0.00680	25.0
Trim Drag	$C_{D_{trim}}$	0.00125	4.6
Compressibility	$C_{D_{P_{fuselage}}}$	0.00090	3.3
	$C_{D_{P_{wing}}}$	0.00179	6.6
Friction	C_{D_F}	0.01650	60.5
Total	C_D	0.02724	100.0

The friction drag is by far the largest contributor to the overall drag. The following is its breakdown:

Friction Drag Component		Drag Coefficient	% of Total
Wing	$C_{D_{F_{wing}}}$	0.00586	35.5
Fuselage	$C_{D_{F_{fus}}}$	0.00813	49.3
Pods	$C_{D_{F_{pods}}}$	0.00134	8.1
Horizontal Tail	$C_{D_{F_{h.t.}}}$	0.00040	2.4
Vertical Tail	$C_{D_{F_{v.t.}}}$	0.00032	1.9
Other	$C_{D_{F_{misc.}}}$	0.00044	2.7
Total	C_{D_F}	0.0165	100

Drag Reduction

The prime candidates for drag reduction by cooling are the wing, the fuselage and the pods. The horizontal and vertical tails in this example do not contribute enough drag to warrant cooling.

Cooling of the wing will be considered only to the hinge lines of the control surfaces. Thus only the forward 75% of the wing will be cooled. A preliminary calculation suggests that only the forward 20% of the fuselage be cooled. Cooling will also be considered for the entire external surface area of the pods. The parameters for the aerodynamic heating calculations are as follows:

$h = 37{,}000$ ft.

$M = 0.85$, $u_e = 822.9$ ft.

$Re/ft = 1.879 \times 10^6$, $Pr = 0.72$

$\rho_e u_e c_p = 4.326$ Btu/ft^2-sec-°F

Component	L_{ft}	ℓ_{ft}	$A_{w_{ft^2}}$	C_{F_ℓ}		C_{D_F}	
				Laminar	Turbulent	Laminar	Turbulent
Wing	20.0	15.0	4440	0.000250	0.00261	0.00043	0.00586
Fuselage	215.5	43.1	2755	0.000147	0.00225	0.00032	0.00813
Pods	16.9	16.9	1536	0.000236	0.00257	0.00012	0.00134

For the purposes of calculation, let us assume that the aircraft has reached cruise conditions before the fuel is circulated for cooling. Thus the aircraft surfaces are initially at the adiabatic wall conditions. In the cooldown process described by equation (5), the coolant must initially remove heat at the turbulent rate. As the surface is cooled, the transition location moves downstream in accordance with the assumption of Figure 5 and so the heat transfer coefficient is reduced but the temperature difference increases. The results of this cooldown calculation are shown in Figure 14. The heat removal rate for each component reaches a maximum during the cooldown process that is well above the final laminar rate (for $x_{tr} = \ell$). Also shown on this figure are the available cooling rates in cruise, in acceleration at h = 10,000 ft. with Mach number going from 0.45 to 0.65 and in climb from 10,000 ft. to 37,000 ft. with the Mach number increasing to 0.85.

It is clear from Figure 14 that the cooling capability is cruise in marginal to inadequate for cooling down the wing or the fuselage under the assumptions of the present calculation. However if the cooldown is done during acceleration or climb there should be no problem in cooling down single components. Cooling all the components simultaneously (Figure 15) does not seem feasible. If methane were to be considered for this example, the cooldown of single components would be marginal even in acceleration.

An estimate of the cooldown time can be made using equation (5). If one assumes a cooled skin structure made of aluminum that has a weight of 2 lb per sq. ft. of skin area and if the available cooling rate is according to the climb curve in Figure 14 then it would take about 3 minutes to cool down the wing, about 2 minutes for the fuselage and under a minute to cool down the pods. It thus seems possible to cool the components consecutively during climb and to maintain the cooled condition for all components together in cruise.

Verification of this last point requires calculating the drag reduction realized by cooling and adjusting the fuel rate for the reduced drag.

The reductions in drag for each component as calculated using equation (11) are shown in Figure 16. The results are also given in the following table:

Component	ΔC_D	% Component Drag	% Friction Drag	% Airplane Drag
Wing	0.0042	72	25	15.4
Fuselage	0.0019	23	12	7.0
Pods	0.0012	90	7.3	4.4

Laminarization by cooling can reduce the drag coefficient by as much as 0.0073 which is 26.8% of the original airplane drag. Cooling only the wing and fuselage results in a 22% reduction for the airplane. It may be concluded that drag reductions of the order of 20% are well within reason. If the fuel rate in cruise is now adjusted downward by 26.8% it is still sufficient to maintain the cooled condition after the cooldown transient as is shown in Figure 15.

Cooling System

The development so far has been a bit simplistic in that the cooling system has thus far been an abstraction. We must now consider the consequences of a real cooling system that has real heat exchangers, pumps, etc.

The cooling system for drag reduction cannot be activated until the aircraft climbs above icing altitudes. Also, the entire cooling capability of the hydrogen may not be needed in cruise. These are but two of the more obvious reasons for having a fuel feed system that can be operated independently of the cooling system and allows the use of a more inert fluid than hydrogen to be circulated as a coolant. The coupling between the fuel and the coolant will be through heat exchangers.

A cooling system for this aircraft application has been suggested by Cunnington[26]. The coolant is gaseous nitrogen. The boiling point of nitrogen is below 200°R at pressures of

interest so that using it as a coolant for surfaces to be brought to 310 - 340°R is quite reasonable. The coolant passages adjacent to the skin surface to be cooled would be integral with the skin as shown in Figure 17. This would tend to minimize the weight penalty of the cooling system. Cunnington estimates the overall weight of the cooling system to be about 4000 lbs.

The net benefits from a drag coefficient reduction of 0.0073 together with a cooling system weight penalty of 4000 lbs. have been calculated using the Lockheed ASSET program with the following results[27]:

Item	Baseline Value	Saving*	
		Amount	Percent
Block fuel (cruise) lb.	50,710	14,100	27.8
Take-off Gross Weight lb.	377,800	28,000	7.4
L/D cruise	16.4	20.9	27**
D.O.C. ¢/seat-n.mi	1.60	0.37	23.1

*Initial evaluation - no iteration
**Percent increase in L/D

If the overall drag reduction were only 0.0054 or 20%, the block fuel saving would be 10,500 lb or 20.7% and the take-off gross weight would be reduced by 19,000 lb. Whether one realizes 26% drag reduction or 20%, the savings certainly make drag reduction by cooling very attractive.

FACTORS REQUIRING FURTHER INVESTIGATION

There are many premises underlying the concept developed in this paper that require substantiation. Further work is required on the stability and transition of three-dimensional compressible flows over aerodynamic surfaces. Stability calculation procedures now being developed for incompressible flow have to be extended to the compressible domain. Equally important is the undertaking of careful experiments on boundary layer transition on swept wings so that other factors - roughness, for example - can be studied. Such experiments should be carried out in a low turbulence wind tunnel whose disturbance environment is measured and known. Clearly more thought must be given to the cooling system design and to internal insulation requirements so that the cooling is effective where it is supposed to be and nowhere else.

Not considered in this paper but quite important is the development of guidelines for structural design that are compatible with the special thermal requirements of the cooled aircraft.

Finally additional configuration studies should be performed to determine the extent of the flight domain for which the effect of cooling is favorable. Trends are difficult to predict reliably because of the many interrelated factors involved.

CONCLUDING REMARKS

The prospects for drag reduction by cooling for cryo-fueled aircraft have been examined. It has been found that this technique is more suited to hydrogen than to methane. Calculations for a M = 0.85 hydrogen fueled aircraft show that drag reductions of the order of 20% are within reason and provide significant fuel savings. These results are such as to justify further investigation of the various elements of this drag reduction phenomenon, and the factors affecting its practical application; for they indicate that the hydrogen fueled aircraft is an attractive candidate for an energy conservative aircraft that uses an alternative fuel.

ACKNOWLEDGEMENT

The author gratefully acknowledges numerous interesting and productive conversations with Mr. G. Daniel Brewer of the Lockheed California Company and wishes to thank Dan Brewer and George Cunnington of Lockheed for supplying unpublished information that was included in this paper.

REFERENCES

1. Brewer, G. Daniel: The Case for Hydrogen-Fueled Transport Aircraft. Astronautics and Aeronautics, Vol. 12, No. 5, May 1974, pp. 40-51.
2. Mikolowsky, William T., Noggle, Larry W. and Stanley, William L.: The Military Utility of Very Large Airplanes and Alternative Fuels. Astronautics and Aeronautics, Vol. 15, No. 9, September 1977, pp. 46-56.
3. Mack, L.M.: Transition Prediction and Linear Stability Theory. Proceedings AGARD Conference on Laminar-Turbulent Transition. AGARD CP-224, pp. 1-1 to 1-22, 1977.
4. Benney, David J. and Orszag, Steven A.: Stability Analysis for Laminar Flow Control, Part I. NASA CR-2910, October 1977.
5. Srokowsky, Andrew J. and Orszag, Steven A.: Mass Flow Requirements for LFC Wing Design. AIAA Paper 77-1222, presented at AIAA Aircraft Systems and Technology Meeting, August 1977.
6. Mack, Leslie M.: Three-Dimensional Effects in Boundary Layer Stability. Proceedings 12th Symposium on Naval Hydrodynamics, June 1978.
7. Frick, C.W., Jr. and McCullough, G.B.: Tests of a Heated Low Drag Airfoil, NACA ARR, Dec. 1942.
8. Liepmann, H.W. and Fila, G.H.: Investigations of Effects of Surface Temperature and Single Roughness Elements on Boundary Layer Transition. NACA Report 890, 1947.
9. Lees, Lester: The Stability of the Laminar Boundary Layer in a Compressible Fluid. NACA Report 876, 1947.

10. Boehman, L.I. and Mariscalco, M.G.: The Stability of Highly Cooled Compressible Laminar Boundary Layers. AFFDL-TR-76-148, December 1976.
11. Kachanov, Y.S., Koslov, V.V. and Levchenko, V. Ya.: Experimental Study of the Influence of Cooling on the Stability of Laminar Boundary Layers. Izvestia Sibirskogo Otdielenia Ak. Nauk SSSR, Seria Technicheskikh Nauk, Novosibirsk, No. 8-2, pp. 75-79, 1974.
12. Gaponov, S.A. and Maslov, A.A.: Izvestia Sibirskogo Otdielenia Ak. Nauk SSSR, Seria Technicheskikh, Novosibirsk, No. 3-1, 1971.
13. Schubauer, G.B. and Skramstad, H.K.: Laminar Boundary Layer Oscillations and Transition on a Flat Plate, NACA Report 909, 1948.
14. Ross, J.A., Barnes, F.H., Burns, J.G. and Ross, M.A.S.: The Flat Plate Boundary Layer. Part 3. Comparison of Theory with Experiment, J. Fluid Mech., Vol. 43, pp. 819-832, October 1970.
15. Strazisar, A., Reshotko, E. and Prahl, J.M.: Experimental Study of the Stability of Heated Laminar Boundary Layers in Water. J. Fluid Mech., Vol. 83, pp. 225-247, Dec. 1977.
16. Smith, A.M.O. and Gambaroni, N.: Transition, Pressure Gradient and Stability Theory, Report ES 26388, Douglas Aircraft Co., 1956.
17. van Ingen, J.L.: A Suggested Semi-Empirical Method for the Calculations of the Boundary Layer Transition Region. Report VTH-74. Dept. of Aero. Eg'g., University of Technology, Delft, 1956.
18. Wazzan, A.R. and Gazley, C. Jr.: The Combined Effects of Pressure Gradient and Heating on the Stability and Transition of Water Boundary Layers. Proc. 2nd Int. Conf. on Drag Reduction, BHRA, Cambridge, Sept. 1977, Paper E3.
19. Reshotko, E.: Drag Reduction in Water by Heating. Proceedings 2nd International Conference on Drag Reduction, Paper E2, BHRA, Sept. 1977.
20. Reshotko, E. and Beckwith, I.E.: Compressible Laminar Boundary Layer over a Yawed Infinite Cylinder with Heat Transfer and Arbitrary Prandtl Number. NACA Report 1379, 1958.
21. Owen, P.R. and Randall, D.G.: Unpublished work quoted in L. Rosenhead, ed., Laminar Boundary Layers, Oxford, 1963, pp. 554-5.
22. Beckwith, Ivan E.: Similar Solutions for the Compressible Boundary Layer on a Yawed Cylinder with Transpiration Cooling. NACA TN 4345, 1958.
23. Pfenninger, W. and Reed, V.D.: Laminar Flow Research and Experiments. Astronautics and Aeronautics, Vol. 4, No. 7, pp. 44-50, July 1966.
24. Poll, D.I.A.: Leading Edge Transition on Swept Wings. AGARD Conf. on Laminar-Turbulent Transition. AGARD-CP-224,May 1977, pp. 21-1 to 21-11.
25. Brewer, G.D., Morris, R.E., Lange, R.H. and Moore, J.W.: Study of the Application of Hydrogen Fuel to Long-Range Subsonic Transport Aircraft. Vol. II, Final Report, NASA CR-132559, January 1975.
26. Cunnington, George: Lockheed Space and Missile Co. Private Communication, Jan. 1978.
27. Brewer, G.D.: Lockheed California Co. Private Communication, Jan. 1978.

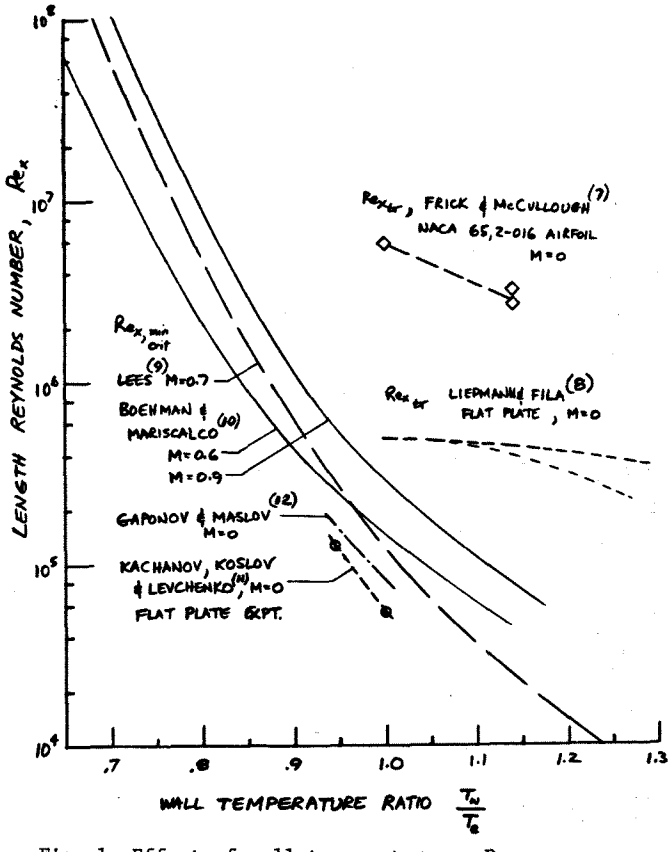

Fig. 1 Effect of wall temperature on $Re_{x_{min\ crit}}$ and on $Re_{x_{tr}}$ as taken from the literature.

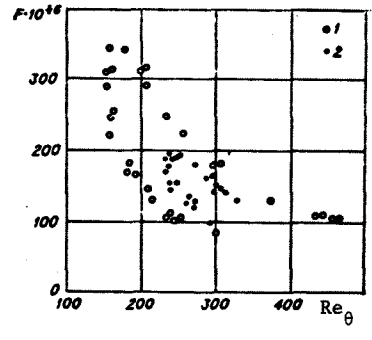

Fig. 2 Points on neutral curve for insulated and cooled plates. 1 - insulated plate, 2 - cooled plate, $T_w/T_e = 0.945$ (from Kachanov, Koslov and Levchenko(11)).

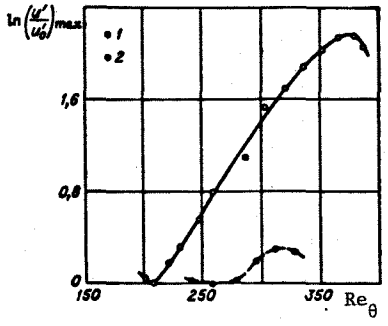

Fig. 3 Growth of disturbance of dimensionless frequency F = 128 x 10^{-6}. 1 - Insulated plate, 2 - cooled plate, T_w/T_e = 0.945 (from Kachanov, Koslov and Levchenko[11]).

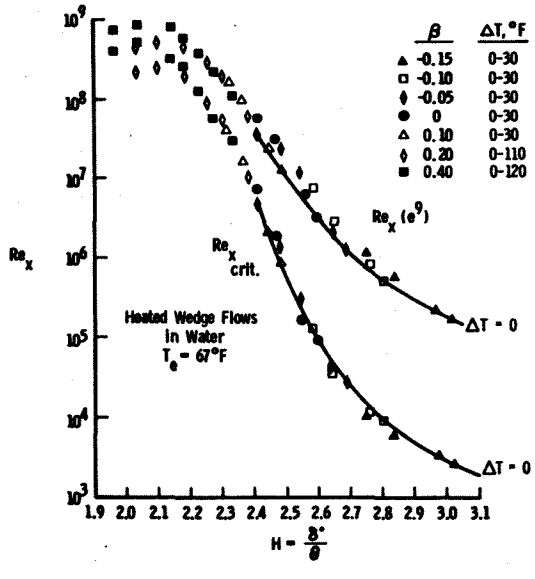

Fig. 4 Minimum critical Reynolds number and predicted transition Reynolds numbers for unheated and heated wedge flows in water (from Wazzan and Gazley[18]).

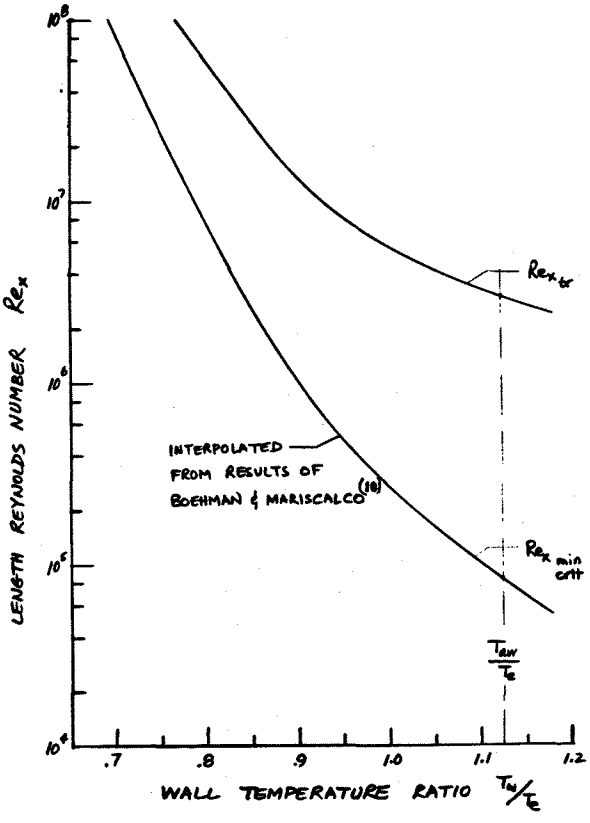

Fig. 5 Assumed transition Reynolds number variation M = 0.85.

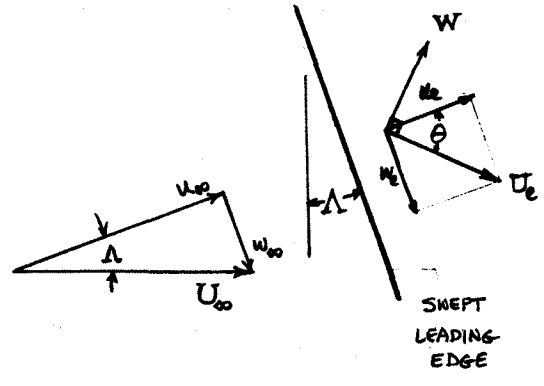

Fig. 6 Geometry of the cross flow

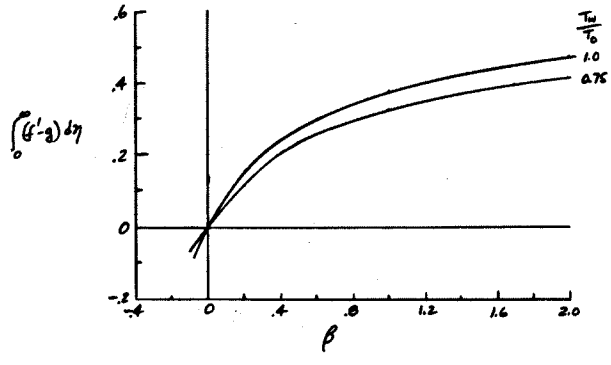

Fig. 7 Crossflow profile integral

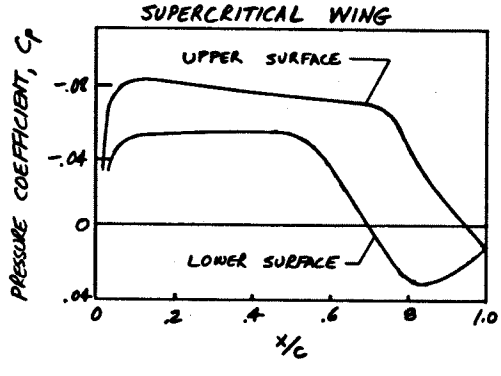

Fig. 8 Representative pressure distribution for supercritical wing at high subsonic Mach number.

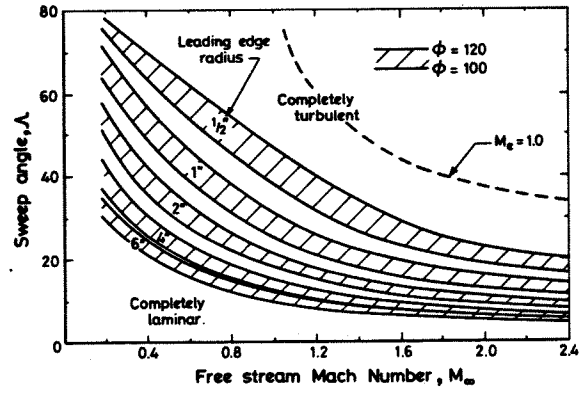

Fig. 9 Transition region boundaries for a 12% thick RAE 101 airfoil section with gross leading edge contamination and zero heat transfer at h = 35000 ft. (from Poll[24]).

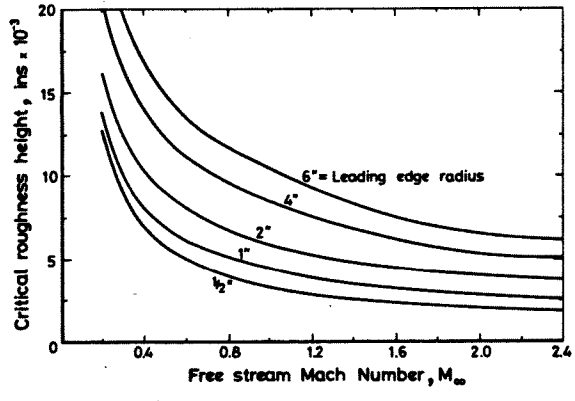

Fig. 10 Minimum trip wire diameter which will induce transition at ϕ = 100 on a 12% thick RAE 101 airfoil section with zero heat transfer at h = 35000 ft. (from Poll[24]).

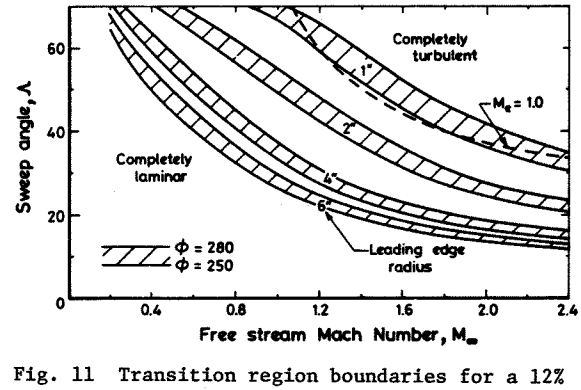

Fig. 11 Transition region boundaries for a 12% thick RAE 101 airfoil section with a smooth leading edge and zero heat transfer at h = 35,000 ft. (from Poll[24]).

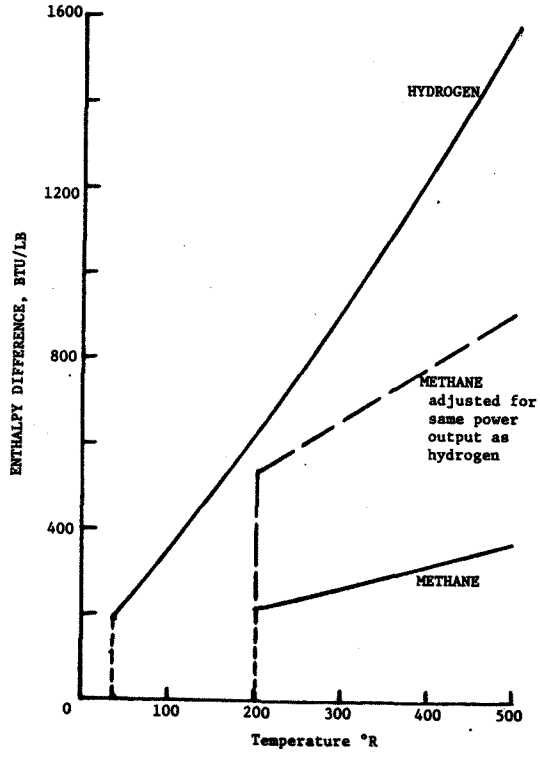

Fig. 12 Enthalpy above saturated liquid conditions for hydrogen and methane.

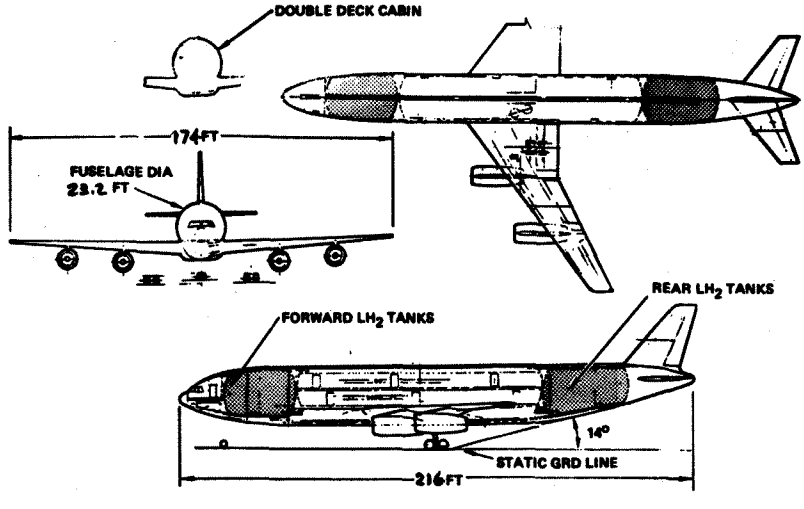

Fig. 13 General arrangement, LH_2 subsonic transport (from Brewer).

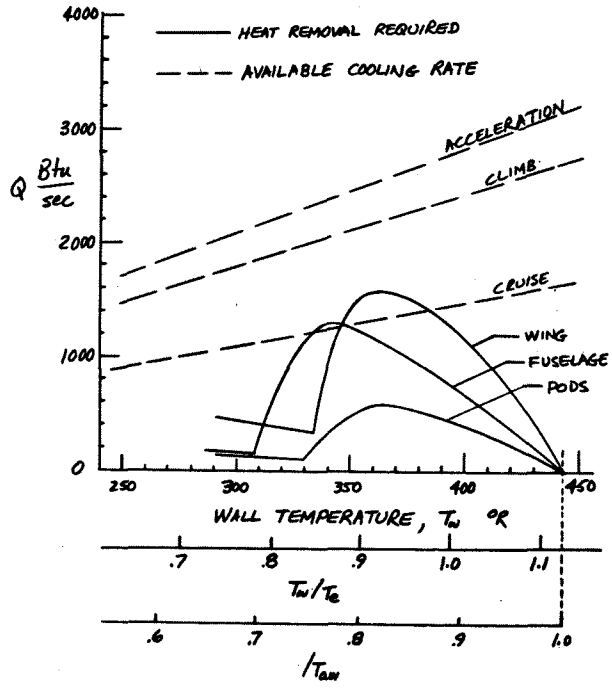

Fig. 14 Heat removal required during cooldown vs. available cooling rates for LH_2 fuel - individual components.

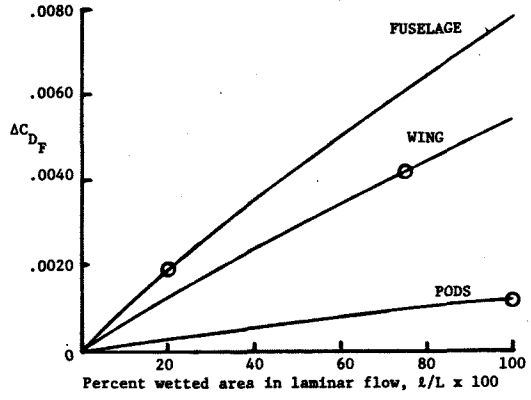

Fig. 16 Drag coefficient reduction due to cooling.

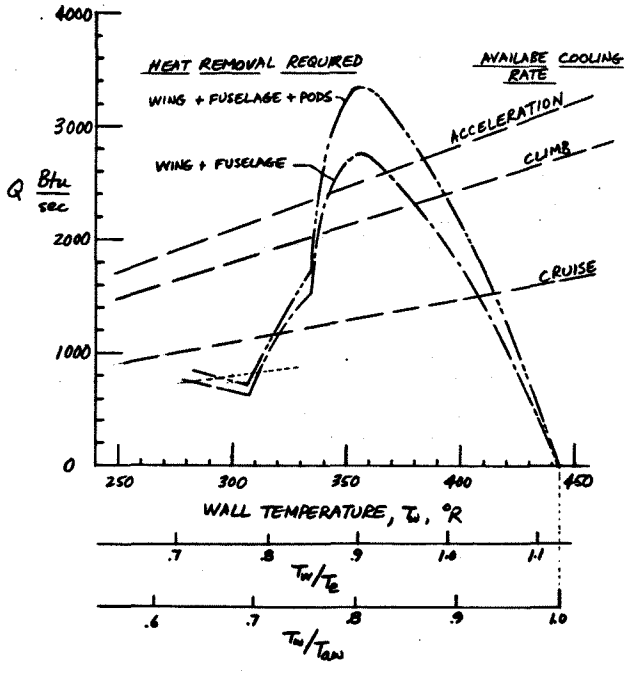

Fig. 15 Heat removal required during cooldown vs. available cooling rates for LH_2 fuel - components cooled simultaneously.

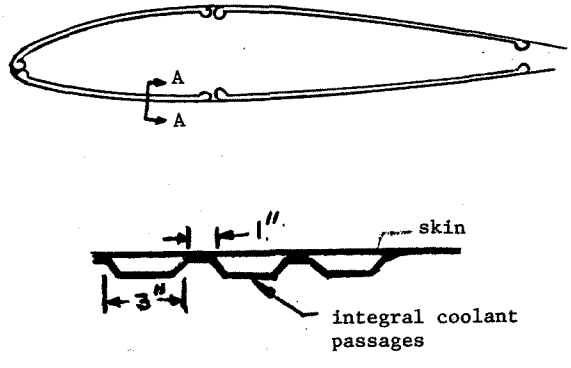

section A-A

Fig. 17 Schematic of skin cooling arrangement (from Cunnington[26]).